

Aerodynamic/Acoustic Splitting Technique for Computational Aeroacoustics Applications at Low Mach Numbers

W. De Roeck,* M. Baelmans, and W. Desmet
Katholieke Universiteit Leuven, 3001 Leuven, Belgium

DOI: 10.2514/1.31953

Hybrid computational aeroacoustics applications approaches, in which the computational domain is split into an aerodynamic source domain and an acoustic propagation region, are commonly used for aeroacoustic engineering applications and have proven to be of acceptable efficiency and accuracy. The different coupling techniques tend to give erroneous results for a number of applications, which are mainly encountered in confined environments. Acoustic analogies are inaccurate if the acoustic variables are of the same order of magnitude as the flow variables, and an acoustic continuation of the source-domain simulation using the latter solution as acoustic boundary conditions is only possible if no vortical outflow is occurring. These inaccuracies can be avoided by using appropriate filtering techniques in which the source-domain solution is split into an acoustic and an aerodynamic fluctuating part. In this paper, such an aerodynamic/acoustic splitting technique is developed and validated for some simple test cases. The filtering method is valid for low-Mach-number applications, assuming that all compressibility effects are caused by the irrotational acoustic field and that the incompressible aerodynamic field is responsible for the vortical movement of the flowfield. Under these assumptions, it is shown that the aerodynamic and acoustic fields at every time step are obtained by solving a system of Poisson equations driven by the fluctuating expansion ratio and vorticity, obtained from the source-domain simulation. For hybrid computational aeroacoustics applications approaches, this filtering technique, generally applicable for both free-field and confined-flow applications, provides more accurate coupling information and improves the knowledge of aerodynamic-noise-generating mechanisms.

Nomenclature

A_{ac}	=	acoustic system matrix
A_t	=	aerodynamic system matrix
c_0	=	speed of sound
L	=	Lamb vector
M	=	Mach number
p	=	pressure
r, θ, φ	=	spherical coordinates
T_{ij}	=	Lighthill stress tensor
t	=	time
u	=	velocity vector
u_i	=	velocity component
V	=	propagation speed of the acoustic waves
x_i	=	spatial coordinate
Δ	=	expansion ratio
δ_{ij}	=	Kronecker delta
ρ	=	density
τ_{ij}	=	viscous tensor
ϕ	=	velocity potential
χ	=	vector potential
ω	=	vorticity vector

Subscripts

$(\cdot)_{ac}$	=	acoustic fluctuating value
$(\cdot)_t$	=	turbulent fluctuating value
$(\cdot)_0$	=	time-averaged value

Superscript

$(\cdot)'$	=	fluctuating value
------------	---	-------------------

I. Introduction

AEROACOUSTICS is a research area of growing interest and importance over the last decade. In the transportation sector, the interest for this field has emerged during the last few years, for various reasons. In aeronautics, for example, strict noise regulations around airports are forcing aircraft manufacturers to reduce the noise emissions during landing and takeoff operations. In the automotive industry, customer surveys identify wind noise as a regular complaint.

With the increase in computational power, the direct computation of aerodynamic noise has become feasible for academic cases [1–3]. Such a direct approach solves the compressible Navier–Stokes equations, which describe both the flowfield and the aerodynamically generated acoustic field. Because of the large disparity in energy and length scales between the acoustic variables and the flow variables that generate the acoustic field, and because acoustic waves propagate over large distances, the direct solution of the Navier–Stokes equations for computational aeroacoustics (CAA) problems is only possible for a limited number of engineering applications [4].

To meet the required design times without excessive costs, hybrid methods are proposed. In these methods, the computational domain is split into different regions, such that the governing flowfield (source region) or acoustic field (acoustic region) can be solved with different equations, numerical techniques, and computational grids. As such, the prediction of the acoustic field at large distances from the sound source is enabled. There are a large number of hybrid methodologies, differing from each other in the type of applied propagation equations or in the way the coupling between source region and propagation region is established.

The classical linear acoustic wave equation and the convective wave equation can be used as acoustic propagation equations [5]. Both of them make assumptions about the mean flowfield: the acoustic wave equation assumes no mean flow, whereas the convected wave equation can only be used when an irrotational mean

Presented as Paper 3726 at the 13th AIAA/CEAS Aeroacoustics Conference, Rome, 21–23 May 2007; received 4 May 2007; revision received 21 September 2007; accepted for publication 7 November 2007. Copyright © 2007 by the American Institute of Aeronautics and Astronautics, Inc. All rights reserved. Copies of this paper may be made for personal or internal use, on condition that the copier pay the \$10.00 per-copy fee to the Copyright Clearance Center, Inc., 222 Rosewood Drive, Danvers, MA 01923; include the code 0001-1452/08 \$10.00 in correspondence with the CCC.

*Ph.D., Department of Mechanical Engineering, Celestijnenlaan 300B; wim.deroeck@mech.kuleuven.be. Member AIAA.

flow is present. In most engineering applications, these assumptions do not hold and more advanced propagation models are needed that are based on a linearization of the Euler equations [6–8]. These equations can be used for most types of mean flow.

The coupling methods that are commonly used for hybrid CAA applications can be divided roughly into two categories: one based on equivalent source formulations and the other based on an acoustic continuation of the source-region simulation.

The idea of using equivalent aeroacoustic sources was first introduced by Lighthill [9,10] and was later formulated by, among others, Curle [11], Ffowcs-Williams and Hawkings [12], Powell [13], and Howe [14]. By rewriting the Navier–Stokes equations in such a way that the left-hand side equals the linear acoustic wave equation with the density as an acoustic variable, the well-known Lighthill stress tensor is obtained as an aeroacoustic source term on the right-hand side. This idea has since been widely used many other types of propagation equations. It is shown further in this paper that acoustic analogies fail to give accurate results for applications in which the acoustic variables become of the same order of magnitude as the aerodynamic fluctuations, which is the case when the acoustic field is generated by a flow-acoustic feedback coupling (e.g., cavity noise) or when acoustic modes are present (e.g., duct aeroacoustics). With a filtering of the source-region results into an acoustic part and a purely aerodynamic part, it should be possible to avoid these drawbacks.

The other coupling method, based on an acoustic continuation of the source-domain simulation, assumes that the acoustic variables on a surface surrounding the source region (Kirchhoff's surface) can be obtained from a proper flow-domain simulation. This acoustic information can then be used as a specific type of coupling boundary condition for the various propagation equations [12,15], resulting in an acoustic continuation of the source-region calculation. However, when a vortical flow passes through Kirchhoff's surface, aerodynamic fluctuations cause hydrodynamic pressure fluctuations, also known as pseudosound, to be present in the propagation region. This can result in nonphysical or even unstable acoustic solutions in the downstream region. It is clear that proper filtering techniques are needed to avoid these errors. The theoretical development of such filtering procedures is elaborated in the present paper.

The next section of this paper discusses the different coupling techniques and illustrates the need for filtering techniques for hybrid CAA methodologies. In the following section, the theoretical framework is developed for a general filtering technique, based on an aerodynamic/acoustic splitting approach, for subsonic CAA applications. This approach is validated for two academic test cases involving both a confined and a free-field application. The main conclusions are summarized in the final section.

II. Coupling Techniques for Hybrid CAA Methodologies

A. Acoustic Analogies

Lighthill [9] introduced the use of acoustic analogies. By rewriting the Navier–Stokes equations in such a way that the left-hand side equals the linear acoustic wave equation without a mean flow and all other terms are treated as source terms on the right-hand side, Lighthill obtained the stress tensor T_{ij} as an equivalent source term for subsonic isentropic flows:

$$\frac{\partial^2 \rho}{\partial t^2} - c_0^2 \nabla^2 \rho = \frac{\partial^2 T_{ij}}{\partial x_i \partial x_j} \quad (1)$$

where T_{ij} is defined as

$$T_{ij} = \rho u_i u_j + (p - c_0^2 \rho) \delta_{ij} - \tau_{ij} \quad (2)$$

If viscous and heat-conducting effects are neglected, the Lighthill stress tensor is simplified to

$$T_{ij} \simeq \rho u_i u_j \quad (3)$$

which can be further simplified to $\rho_0 u_i u_j$ for low-Mach-number applications, because it is known that density changes are of the order of M^2 . The approach of replacing the whole noise-generating flowfield by an equivalent source term is appealing due to its simplicity and can be used to identify possible aeroacoustic source phenomena.

The approach of Lighthill [9] is correct as long as the velocity components u_i do not contain any acoustic fluctuations. If this is not the case, each isentropic flow variable f can be decomposed into a mean part f_0 , an aerodynamic or turbulent fluctuating part f'_t , and an acoustic fluctuating part f'_{ac} , which allows us to rewrite the Lighthill stress tensor as

$$\begin{aligned} T_{ij} &\simeq \rho u_i u_j \\ &\simeq (\rho_0 + \rho'_t + \rho'_{ac})(u_{i0} + u'_{i,t} + u'_{i,ac})(u_{j0} + u'_{j,t} + u'_{j,ac}) \quad (4) \end{aligned}$$

Chu and Kovácszay [16] identified only the term $\rho_0(u_{i0} + u'_{i,t})(u_{j0} + u'_{j,t})$ as the aerodynamic generation of acoustic waves, based on a study of the nonlinear interactions in a viscous heat-conducting compressible gas. All other terms are of a different nature and cannot be considered as sources of sound. For example, the terms $\rho_0 u'_{i,ac} u'_{j,ac}$, $\rho_0 u_{i0} u'_{j,ac}$, and $\rho_0 u'_{i,t} u'_{j,ac}$ represent, respectively, the nonlinear acoustic contributions, a convective effect of the acoustic waves, and an interaction between the acoustic and the vorticity mode. These terms should ideally be omitted in the source-term formulation to obtain an accurate representation of the noise-generating mechanism.

For applications in which the acoustic velocity fluctuations are negligible in comparison with the turbulent velocity fluctuations or when carried out in an incompressible way, the source-region simulation allows us to describe the Lighthill source terms directly. This assumption, however, does not hold for most confined-flow applications, in which acoustic resonances may occur and/or a feedback coupling between the acoustic field and aerodynamic field may be present. In this case, the source-region results should ideally be decomposed into an acoustic fluctuating part and a turbulent fluctuating part, the latter necessary for an accurate source-term representation.

Ewert and Schröder [7] proposed to modify the wave operator to include the convective acoustic terms in the left-hand side. Because the acoustic waves can be assumed to be irrotational, an irrotational formulation of the linearized Euler equations (LEE), the acoustic perturbation equations is obtained. Furthermore, they applied a filtering of the source term such that only the acoustic modes are excited. In this way, they obtained an aerodynamic sound source-term formulation based on the fluctuating Lamb vector $\mathbf{L}' = (\boldsymbol{\omega} \times \mathbf{u})'$, similar to the acoustic analogies based on the theory of vortex sound [13,14,17]. Because the acoustic field can be assumed to be irrotational ($\boldsymbol{\omega}_{ac} = 0$), this source-term formulation does not contain any nonlinear effects of the acoustic field. A small, no-noise-generating, convective effect ($\boldsymbol{\omega}_0 \times \mathbf{u}_{ac}$) and a term originating from the interaction between the aerodynamic and acoustic fields ($\boldsymbol{\omega}_t \times \mathbf{u}_{ac}$) are still present, however. A splitting of the source-domain results into an acoustic and a turbulent fluctuating part would, in this case, also improve the accuracy of this source-term formulation. A possible splitting procedure of the velocity fluctuations into their aerodynamic and acoustic fluctuating parts is proposed in Sec. III.

B. Acoustic Continuation of the Source-Domain Simulation

The basic principle of the acoustic analogy is replacing the source region with an equivalent source distribution. An alternative to this approach is obtained when the source-region simulation is performed in a compressible way and with high accuracy, such that acoustic waves propagating in the source region are present in the final source-domain results [15]. In this case, the source domain is coupled directly with the propagation region using the acoustic information on a surface surrounding the most important sources (the Kirchhoff surface) as boundary input for the acoustic simulation.

A coupling procedure based on this transfer of direct acoustic boundary information has the following advantages over the acoustic analogy approach:

1) Because there is no information inside the source region needed for this coupling technique, the acoustic region does not contain the source region, resulting in a smaller computational acoustic domain.

2) This coupling technique can be seen as an acoustic continuation of the source-domain simulation. If the acoustic fluctuations on the Kirchhoff surface are accurately predicted, it can be expected that this technique yields more accurate results [18].

3) In contrast to the acoustic analogy theory, no assumptions are made toward the noise-generating mechanisms, and thus no equivalent source-term formulations are required.

4) The acoustic fluctuations are only needed on a surface surrounding the source region, which reduces the storage requirements compared with the equivalent sources, which often require information over the whole volume of the source region.

The major disadvantages of this coupling procedure are as follows:

1) The source-region simulation needs to be compressible and the results need to be of high accuracy. As a result, CAA techniques that are commonly used for direct noise simulations are needed, resulting in computationally demanding simulations.

2) If vortical outflow occurs through the coupling interface, the fluctuating variables may contain aerodynamic fluctuations that are of much larger amplitude than the acoustic fluctuations and may generate spurious hydrodynamic pressure fluctuations inside the acoustic field [19]. A filtering of the source-domain fluctuations into an acoustic and aerodynamic part is thus needed to obtain meaningful acoustic results when an outflow through the Kirchhoff surface is occurring.

3) All aerodynamic sources should be located inside the Kirchhoff surface and, especially when vortical outflow is likely to occur, the source region can become relatively large.

4) Because the acoustic domain does not contain the source region, all acoustic effects, including the excitation of purely acoustic resonances of the system, have to be present in the acoustic information on the Kirchhoff surface. If acoustic resonances are only weakly excited, this information may be masked by the aerodynamic pressure fluctuations and, as a result, may not be incorporated in the far-field acoustic results. Because the acoustic propagation region contains the source region, for a coupling strategy based on equivalent aeroacoustic sources, a possible excitation of acoustic resonances is, by definition, included in the acoustic simulation.

An improvement of this coupling technique can be obtained by applying a mode-matching strategy [20] on the source-domain results. The technique uses a small matching interface between the source region and the acoustic region, consisting of three or more axial planes. At the matching interface, the acoustic pressure fluctuations are obtained through a least-squares fit of the pressure fluctuations obtained in the source region with the acoustic modes of the duct. This method is often referred to as the multiple-plane-matching technique.

This technique is appealing due to its simplicity and ease of implementation. Some successful validations have been performed in the European Turbo Noise CFD project [21] for the acoustic propagation of aeroacoustic sources in turbofan engine bypass ducts. Furthermore, a distinction between the right- and left-running acoustic waves can be made, which makes it possible to exclude the reflected modes from the solution, making this method less sensitive to the boundary conditions used for the source-domain computation. However, this approach has only a limited number of applications in which the acoustic pressure fluctuations dominate the hydrodynamic pressure fluctuations and for applications that mathematically allow a representation of the solution by slowly varying modes [22]. This filtering technique is useful for applications with a confined uniform mean flow and in which acoustic pressure fluctuations are dominant. In a large number of low-Mach-number applications, it can be expected that acoustic pressure fluctuations are of low amplitude and are hence difficult to obtain from the total pressure field in the source region with this filtering technique.

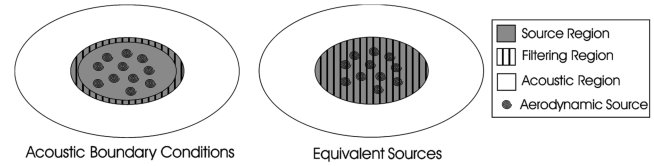


Fig. 1 Overview of the filtering region for hybrid CAA techniques based on a coupling through acoustic boundary conditions (left) and equivalent aeroacoustic sources (right).

III. Aerodynamic/Acoustic Splitting Technique

From the discussion of the different coupling strategies, it is clear that a splitting of the source-domain results into an aerodynamic and an acoustic fluctuating part is needed to improve the accuracy of hybrid CAA simulations, for the following reasons:

1) A coupling strategy using equivalent aeroacoustic source formulations may contain a spurious contribution from the fluctuating acoustic part when the acoustic fluctuating variables are not negligible when compared with the aerodynamic fluctuations. This is the case, for instance, if acoustic resonances are likely to occur or when a flow-acoustic feedback coupling is present.

2) When using an acoustic continuation of the source-region simulation as a coupling technique and when a turbulent flow passes the Kirchhoff surface, the fluctuating boundary values may contain a spurious contribution from the aerodynamic fluctuating field when the latter is not negligible when compared with the acoustic fluctuations.

For hybrid CAA simulations in confined flows, neither of the coupling techniques is thus able to provide a reliable and accurate aeroacoustic input for the propagation equations, and a filtering procedure, as illustrated in Fig. 1, is needed with the following general properties:

1) The filtering procedure should obtain both the aerodynamic fluctuating part and the acoustic fluctuating part that are needed for, respectively, the equivalent source approach and the Kirchhoff surface variables.

2) The splitting of the source-domain results should yield filtered variables over the whole source-region volume (equivalent sources) or over a small surface (acoustic boundary condition).

3) The technique should be generally applicable for confined and free-field applications.

4) The applicability range of the filtering method should cover both large and small ratios of the aerodynamic-to-acoustic fluctuations.

5) To reduce the data handling and storage requirements, a time-domain formulation is preferable, because in this way, the filtering technique can be incorporated inside the source-domain solver.

As previously discussed, mode-matching strategies only result in acoustic frequency-domain information on a small region of a confined computational domain in which the acoustic modes are known. As such, they do not satisfy all the required properties that are needed for general-purpose hybrid CAA approach. For this reason, a new aerodynamic/acoustic splitting technique [23] is developed and validated for some simple test cases.

A number of other techniques exist to improve the accuracy of the hybrid CAA methods when vortical outflow is occurring. Wang et al. [24] suggested a boundary-correction term for unaccounted sources when vortices convect out of the source region, and Shur et al. [25] used space-averaging over multiple outlet surfaces to avoid hydrodynamic pressure oscillations, which can be assumed to be randomly distributed at high-Reynolds-number flows. These methods are not filtering techniques, because they do not allow a distinction to be made between the aerodynamic and the acoustic fluctuating field. They can be used in combination with the aerodynamic/acoustic splitting technique to further improve the accuracy of the coupling strategies when vortical outflow is occurring.

The aerodynamic/acoustic splitting technique is based on a decomposition of the isentropic velocity fluctuations u' into an aerodynamic or turbulent fluctuating part u'_t and an acoustic

fluctuating part \mathbf{u}'_{ac} at every time step of the source-region calculation. The choice of using the velocity rather than the pressure fluctuations as filtering variables is motivated by the fact that hydrodynamic pressure fluctuations are present to sustain the vortical fluid motion, and thus knowledge about the aerodynamic velocity field is required to obtain information about this fluctuating hydrodynamic pressure field.

It is well known [26] that each velocity field \mathbf{u}' can be written as the sum of an irrotational \mathbf{u}'_{ac} , a solenoidal \mathbf{u}'_t , and a both solenoidal and irrotational field \mathbf{v}' :

$$\mathbf{u}' = \mathbf{u}'_{ac} + \mathbf{u}'_t + \mathbf{v}' \quad (5)$$

where it can be assumed that the fluctuating solenoidal and irrotational field is negligibly small ($\mathbf{v}' = 0$).

A. Field Description

From a compressible source-region simulation, the total velocity fluctuations \mathbf{u}' are known and they describe all nonlinear interactions occurring between the aerodynamic and acoustic fields. As with the study of nonlinear interactions in a fluid by Chu and Kovásznyai [16], a distinction between the acoustic and aerodynamic field can be made for an isentropic low-Mach-number flowfield.

1. Acoustic Field

For low-Mach-number aeroacoustics applications, it can be assumed that the aerodynamic field is incompressible, and thus all compressibility effects that are incorporated in the fluctuating dilatation rate $\Delta' = \nabla \cdot \mathbf{u}'$ are of a purely acoustic nature. Furthermore, it can be expected that the acoustic field is irrotational, which leads to the following mathematical description of the acoustic velocity fluctuations \mathbf{u}'_{ac} :

$$\begin{cases} \nabla \cdot \mathbf{u}'_{ac} = \nabla \cdot \mathbf{u}' = \Delta' \\ \nabla \times \mathbf{u}'_{ac} = 0 \end{cases} \quad (6)$$

An irrotational velocity field is uniquely described by a velocity potential ϕ , which allows us to simplify the description of the acoustic velocity field into one single Poisson equation:

$$\nabla^2 \phi = \Delta' \quad (7)$$

where $\nabla \phi = \mathbf{u}'_{ac}$. Because the fluctuating dilatation ratio Δ' is known from the source-region calculation, the acoustic velocity field can be obtained numerically when the appropriate boundary conditions are applied to this Poisson equation.

At solid boundaries, the acoustic velocity normal to the wall is zero, which imposes a zero gradient of the acoustic potential in the direction normal to the wall. At the boundaries at which acoustic waves enter or leave the filtering region, the asymptotic radiation boundary conditions of Tam and Dong [27] can be applied to the acoustic potential. In spherical coordinates r , θ , and φ , this leads to the following boundary condition:

$$\frac{1}{V(\theta, \varphi)} \frac{\partial \phi(r, \theta, \varphi, t)}{\partial t} + \frac{\partial \phi(r, \theta, \varphi, t)}{\partial r} + \frac{1}{2r} \phi(r, \theta, \varphi, t) = 0 \quad (8)$$

where the center of the coordinate system is taken at the approximate position of the most important sources, which can be located inside or outside the filtering region, and $V(\theta, \varphi)$ is the propagation speed of the acoustic waves ($c + \mathbf{U}_0 \cdot \mathbf{e}_r$) projected in the r direction.

2. Aerodynamic Field

If the aerodynamic field is assumed to be incompressible, it has a dilatation rate equal to zero. Because the acoustic velocity field is irrotational, all rotational effects of the fluctuating flowfield that are incorporated in the fluctuating vorticity vector $\boldsymbol{\omega}'$ are caused by the aerodynamic velocity field, which allows us to formulate the turbulent fluctuating-velocity field \mathbf{u}'_t as

$$\begin{cases} \nabla \cdot \mathbf{u}'_t = 0 \\ \nabla \times \mathbf{u}'_t = \nabla \times \mathbf{u}' = \boldsymbol{\omega}' \end{cases} \quad (9)$$

This solenoidal velocity field can be described with a vector potential $\boldsymbol{\chi}$. This allows us to formulate the aerodynamic velocity field, similar to the acoustic field, with a system of Poisson equations:

$$\nabla^2 \boldsymbol{\chi} = -\boldsymbol{\omega}' \quad (10)$$

where $\nabla \times \boldsymbol{\chi} = \mathbf{u}'_t$. It should be noted that this is only valid when $\nabla \cdot \boldsymbol{\chi} = 0$, which is the case when the filtering region is a convex domain [26].

As with the acoustic problem, the Poisson equations (10) can be solved numerically when a set of boundary conditions is defined. At solid boundaries, a no-slip boundary condition $\mathbf{u}'_t = \mathbf{0}$ is chosen, and at boundaries at which vortical structures are entering or leaving the computational domain, a mean flow convection of the aerodynamic velocity field is imposed as the following boundary condition:

$$\frac{\partial \boldsymbol{\chi}}{\partial t} + (\mathbf{U}_0 \cdot \nabla) \boldsymbol{\chi} = \mathbf{0} \quad (11)$$

3. Aerodynamic/Acoustic Filtering

Decomposing the total fluctuating-velocity field into an acoustic and a turbulent fluctuating part thus requires solving the following system of Poisson equations:

$$\begin{cases} \nabla^2 \phi = \Delta' \\ \nabla^2 \boldsymbol{\chi} = -\boldsymbol{\omega}' \end{cases} \quad (12)$$

In a two-dimensional velocity formulation, this system of equations can be written as

$$\begin{cases} \frac{\partial u'_{x,ac}}{\partial x} + \frac{\partial u'_{y,ac}}{\partial y} = \Delta' = \frac{\partial u'_x}{\partial x} + \frac{\partial u'_y}{\partial y} \\ \frac{\partial u'_{y,ac}}{\partial x} - \frac{\partial u'_{x,ac}}{\partial y} = 0 \\ \frac{\partial u'_{x,t}}{\partial x} + \frac{\partial u'_{y,t}}{\partial y} = 0 \\ \frac{\partial u'_{y,t}}{\partial x} - \frac{\partial u'_{x,t}}{\partial y} = \boldsymbol{\omega}' = \frac{\partial u'_y}{\partial x} - \frac{\partial u'_x}{\partial y} \end{cases} \quad (13)$$

Although the acoustic and aerodynamic fluctuating-velocity fields are uncoupled in these equations, their mutual interaction is implicitly taken into account through the terms appearing on the right-hand side of the equations. Inside the nonlinear source region, the interaction between the acoustic and aerodynamic velocity fields indeed effects the vorticity and expansion ratio fluctuations. For this reason, it is not necessary to incorporate interaction effects between the filtered aerodynamic and acoustic fields. If the filtering is applied inside the source region, special care is needed when interpreting the filtered variables because they are still subject to a strong mutual interaction, and thus a continuous generation and dissipation is expected.

Once the acoustic potential is determined, the acoustic density and pressure fluctuations ρ'_{ac} and p'_{ac} are obtained through the linearized continuity equation and the isentropic pressure-density relation:

$$\begin{cases} \frac{\partial \rho'_{ac}}{\partial t} + \mathbf{v}_0 \cdot \nabla \rho'_{ac} = -\rho_0 \nabla^2 \phi \\ p'_{ac} = c_0^2 \rho'_{ac} \end{cases} \quad (14)$$

The hydrodynamic pressure fluctuations are known by subtracting these acoustic pressure fluctuations from the total pressure fluctuation, obtained from the source-region simulation.

B. Numerical Implementation

In principle, the aerodynamic/acoustic splitting technique can be implemented using only one Poisson equation. Using, for instance, only the acoustic Poisson equation allows us to determine the acoustic fluctuating field, and the turbulent velocity field is then obtained by the following relation:

$$\mathbf{u}'_t = \mathbf{u}' - \mathbf{u}'_{ac} \quad (15)$$

This approach, although less time-consuming, is not preferable, because the total fluctuating field \mathbf{u}' may contain a contribution from the solenoidal and irrotational field \mathbf{v}' , not taken into account by Eq. (15). Furthermore, the numerical errors introduced by solving the single Poisson equation are inherently present in both variables, especially when one variable is much smaller than the other variables. This may cause inaccurate results. For this reason, an implementation of both Poisson equations is preferred when both the aerodynamic and acoustic fluctuating fields are required. If, on the other hand, only one of the two fluctuating fields is required, a single equation approach can be used without loss of accuracy.

A two-dimensional numerical implementation of the system of equations (12) is carried out using a direct finite difference approach. Two system matrices A_{ac} and A_t with dimension $MN \times MN$ (where M and N are the number of grid points in, respectively, the x and y directions) are constructed for the filtering region. These matrices correspond to the finite difference formulation of the Laplacian for the interior points and the boundary-condition formulation involving first-order space derivatives at the boundary points. The two Poisson equations can be written in this case as

$$A_{ac} \{\phi\} = \{\Delta'\} \quad A_t \{\chi\} = \{\omega'\} \quad (16)$$

where $\{\phi\}$ and $\{\chi\}$ are the vectors containing the MN unknowns and $\{\Delta'\}$ and $\{\omega'\}$ are, respectively, the known fluctuating expansion ratios and vorticity fluctuations in every grid point. Because the system matrices are time-independent and sparse, their inverse can be calculated once with a lower/upper matrix factorization and with fairly high efficiency. The unknown variables at every time step are then obtained with one simple matrix multiplication:

$$\{\phi\} = A_{ac}^{-1} \{\Delta'\} \quad \{\chi\} = A_t^{-1} \{\omega'\} \quad (17)$$

Next to this direct approach, involving the calculation of a matrix inverse, an iterative approach could also be adopted. However, because such an iterative procedure is needed at every time step of the source-region simulation, it can be expected that this iterative implementation is more time-consuming.

For spatial derivatives, a standard fourth-order central-difference scheme is used, and time-advancing (needed for the boundaries through which the acoustic and/or aerodynamic waves are propagating) is carried out using a standard five-stage Runge–Kutta formulation. The efficiency and accuracy of the current numerical implementation can possibly be further improved by using other finite difference schemes or numerical discretization techniques such as the finite element method. Because the goal of this work is the development and the validation of this filtering technique rather than an efficient implementation, this numerical implementation is therefore justified.

The computational cost of the filtering procedure is negligible compared with the source-region simulation time, because it involves (once the inverse system matrices A_{ac}^{-1} and A_t^{-1} are determined) only two matrix multiplications and the Runge–Kutta time-advancing at a limited number of boundary points. Furthermore, because the technique is a time-domain formulation, it can easily be incorporated in a flow-domain solver which allows, without much data handling, to determine a more accurate source-term formulation or purely acoustic boundary conditions.

C. Properties of the Aerodynamic/Acoustic Splitting Technique

The major advantages of the aerodynamic/acoustic splitting technique can be summarized as follows:

The splitting method does not make any assumption toward the size or type of the computational domain. The filtering region can be confined or unbounded and may contain solid surfaces or damping material. The geometrical complexity that can be incorporated is only limited by the numerical discretization technique and the availability of accurate boundary-condition formulations.

Because both the aerodynamic and acoustic fluctuating fields are obtained with this technique, accurate acoustic boundary conditions and source terms can be formulated, especially when a failure of classical hybrid CAA techniques is expected, such as vortical outflow through a Kirchhoff surface or high-amplitude acoustic fluctuations present in equivalent source-term formulations. Because noise-generating mechanisms are implicitly modeled by the right-hand side of the Poisson equations, the filtering region may contain aerodynamic sound sources.

The insight into noise-generating mechanisms is further extended because, especially when a flow-acoustic feedback coupling is present, the noise production can be regarded as an energy transfer between the aerodynamic and acoustic fluctuating fields. Because generation, dissipation, and propagation of both fluctuating fields is present in the filtered results, this technique may help to gain more insight into tonal-aerodynamic-noise-generation mechanisms. Furthermore, the major region in which aerodynamic noise is generated can be identified, which allows us to reduce the computational source domain and, as a result, reduces the computational time of hybrid CAA methods. However, when the filtering technique is applied inside the source region, the resulting aerodynamic and acoustic fields are not straightforward to interpret, because the fluctuations are subject to a mutual interaction. This results in a continuous generation and dissipation of acoustic and/or aerodynamic waves. The filtered results inside the source region may thus not be totally representative for the acoustic far-field radiation.

A Poisson solver is straightforward to implement, and different numerical discretization techniques such as finite element, finite volume, and finite difference techniques can increase the computational efficiency. Furthermore, the system matrix is identical for every time step, which reduces the computational time.

The filtering technique is based on a time-domain formulation that makes it easy to incorporate in CFD solvers, reducing the storage requirements and data handling efforts.

The major disadvantages of the aerodynamic/acoustic splitting technique can be summarized as follows:

Because the filtering strategy assumes that the aerodynamic field is incompressible, the number of applications are limited to low- or moderate-Mach-number flows. The assumption of incompressibility of the aerodynamic field is generally assumed to be valid [28] for Mach numbers below 0.3, based on the turbulent velocity. Although this range can be further extended for certain applications, special care is needed when applying the filter technique for applications in which the Mach number exceeds the value of 0.3.

The final accuracy of the splitting technique largely depends on the accuracy of the fluctuating dilatation ratio and vorticity, which are obtained from the source-region simulation. Especially when the contribution of one of the two fluctuating fields is negligible toward the other, it can be expected that the right-hand side of the Poisson equation may contain a nonnegligible amount of numerical noise, which may contaminate the final filtered aerodynamic and/or acoustic field. A possible increase of the accuracy of the splitting method can be obtained by applying the mode-matching strategies to the filtered acoustic field. Because of the frequency transformation and the least-squares analysis applied in the latter splitting technique, inaccuracies of the acoustic results are filtered out additionally.

If the splitting procedure is used to obtain accurate equivalent source-term formulations, the filter region should include the whole source region. Especially for three-dimensional applications with a large source region, this may result in a large filtering region and, as a consequence, an increase in the total computational time of the hybrid CAA techniques.

IV. Validation of the Aerodynamic/Acoustic Splitting Technique

A first validation of the aerodynamic/acoustic splitting technique focuses on some academic test cases in which no aerodynamic noise sources are present. It involves a confined problem and a free-field problem in which an acoustic field and an aerodynamic field are

artificially superimposed on top of each other and no mutual interactions are occurring.

A. Duct Test Case

The one-dimensional acoustic wave propagation in a two-dimensional straight duct is considered, with a nondimensional height of 20 when a simplified continuous vortex source is present. A velocity field is imposed that consists of an acoustic plane-wave propagation, with a nondimensional wavelength of 10, described by

$$\begin{cases} u'_{ac} = A_{ac} \sin(\frac{2\pi x}{10}) \\ v'_{ac} = 0 \end{cases} \quad (18)$$

and a train of vortices, described by

$$\begin{cases} u'_t = A_t y \exp(0.7(1 - \sqrt{x^2 + y^2})) \\ v'_t = -A_t x \exp(0.7(1 - \sqrt{x^2 + y^2})) \end{cases} \quad (19)$$

is superimposed. The vortices are inserted in the computational domain, with a nondimensional distance of 10 between two adjacent vortices. A_{ac} and A_t are the amplitudes of, respectively, the acoustic and aerodynamic velocity fluctuations. The filtering region consists of 40×40 elements with a nondimensional grid spacing of 0.5, and a uniform mean flow with a Mach number $M_\infty = 0.3$ is imposed. The time-domain velocity fluctuations are obtained by propagating the acoustic and aerodynamic fluctuations with a propagation velocity of, respectively, $c_0 + U_\infty$ and U_∞ . The calculation is performed over

5.000 time steps with a Courant–Friedrichs–Lewy (CFL) number equal to 1.0.

A first calculation is performed with the acoustic and aerodynamic fluctuations at the same order of magnitude: $A_{ac} = A_t = 1$. The instantaneous velocity field at time step 4.000 is shown in Fig. 2. The x component of the velocity u' clearly contains a significant contribution from both velocity fields, whereas velocity fluctuations v' in the y direction only consist of aerodynamic fluctuations, due to the 1D character of the acoustic field.

The first step in the aerodynamic/acoustic splitting technique is the determination of the right-hand side of the equations: the fluctuating expansion ratio Δ' and the vorticity ω' , shown in Fig. 3. Although these terms can easily be obtained in an analytical way in this case, a numerical approach is chosen to include numerical errors introduced by the differentiation of the right-hand-side terms. The expansion ratio Δ' shows a one-dimensional pattern, and the vorticity field contains a periodic train of eddies. It should be noted that numerical differentiation errors of the aerodynamic field may cause a contamination of the fluctuating expansion ratio. Because of the one-dimensional formulation of the acoustic field, resulting in only a nonzero gradient for the x derivative of the u velocity, the opposite effect does not take place.

After applying the previously described wall boundary conditions at the top and lower boundaries and the asymptotic boundary conditions at the upstream and downstream boundaries, the system of Poisson equations is solved numerically. The reconstructed acoustic and aerodynamic velocity fluctuations are shown in Figs. 4–7.

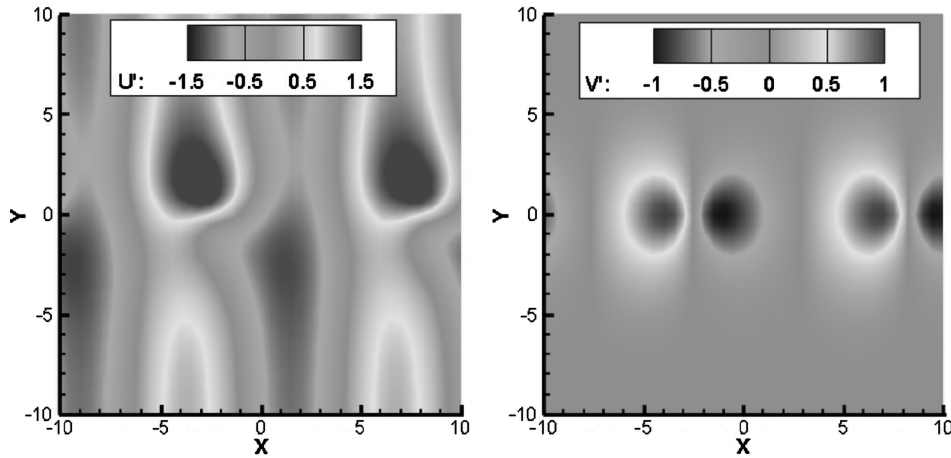


Fig. 2 Total velocity fluctuations of u' (left) and v' (right) at time step 4.000; $A_{ac} = A_t = 1$.

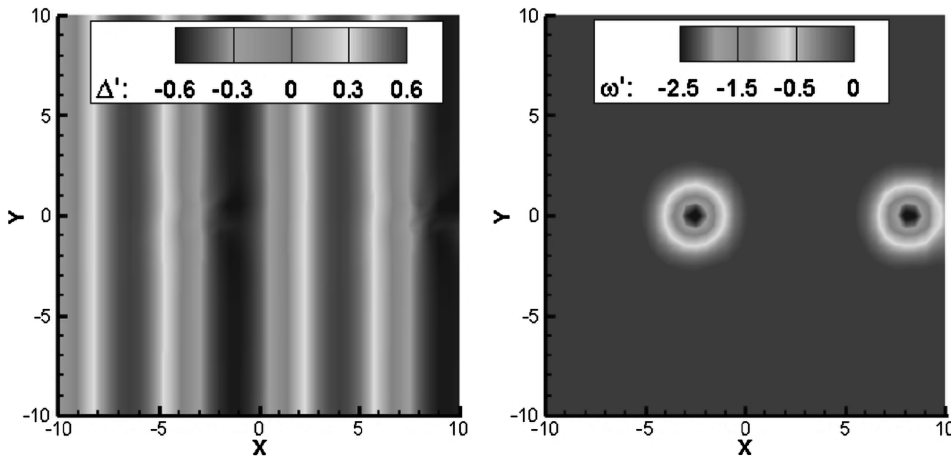


Fig. 3 Expansion ratio Δ' (left) and vorticity ω' (right) of the velocity field at time step 4.000; $A_{ac} = A_t = 1$.

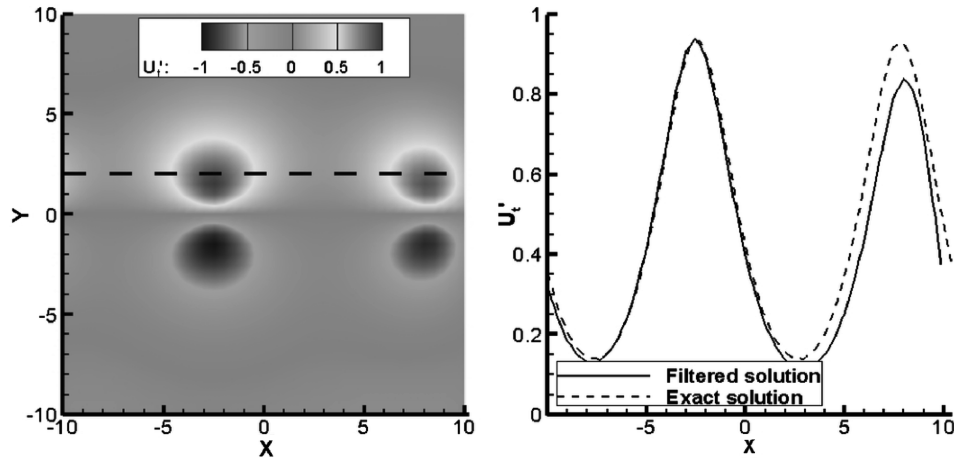


Fig. 4 Filtered aerodynamic velocity fluctuations u'_t in the x direction; contour plot (left) and velocity along line $y = 2.0$ (right) at time step 4.000; $A_{ac} = A_t = 1$.

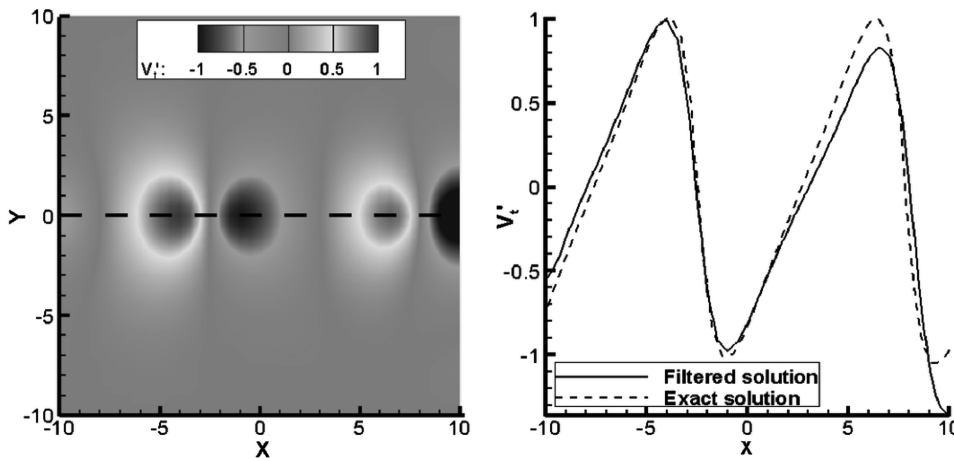


Fig. 5 Filtered aerodynamic velocity fluctuations v'_t in the y direction; contour plot (left) and velocity along line $y = 0.0$ (right) at time step 4.000; $A_{ac} = A_t = 1$.

From Figs. 4 and 5, it is clear that the aerodynamic field is accurately reconstructed, with only a small error introduced near the inflow and outflow boundaries. This can be noticed in the right of the respective figures, in which the filtered aerodynamic velocity profile along a horizontal line is compared with the solution of Eq. (19). The boundary-condition formulation introduces a small amount of damping or amplification in the aerodynamic velocities. After a large number of time steps, however, these errors are not propagated throughout the domain, because the filtering procedure is carried out instantaneously, not using any information of filtered results from previous time steps.

Figure 6 indicates that the acoustic velocity in the x direction is predicted accurately and that some low-amplitude spurious components in the y velocity are present, as shown in Fig. 7. The errors in the vicinity of the radiation boundaries in the acoustic velocities are much smaller than those of the aerodynamic field. The dominant errors in the acoustic y velocity field are located at the position of the vortices for which the centers are located at a nondimensional x position of -2.7 and 7.3 at time step 4.000. This indicates that these errors are originating from the numerical differentiation errors introduced by the aerodynamic contribution to the expansion ratio. Special care is thus needed when computing the right-hand side of the Poisson equations, especially when some fluctuating values are of low amplitude.

For this reason, a more detailed investigation of the influence of the amplitudes A_{ac} and A_t is performed. For this study, the preceding simulation is carried out for a number of situations in which the ratio A_{ac}/A_t varies between 0.0001 and 10,000. The errors of the different

simulations, defined as the rms value of the difference between the analytical and the numerical solution, are shown in Fig. 8. As mentioned before, the aerodynamic velocity fluctuations in this case have no spurious contributions from the numerical errors introduced by the differentiation of the acoustic field, and no decrease in error is observed on the right of Fig. 8. The acoustic velocity field is contaminated by the fact that the numerical calculation of the aerodynamic field's contribution to the dilation rate is not equal to zero. These errors become of growing importance for decreasing values of A_{ac}/A_t .

This effect is further investigated by increasing the order of the finite difference integration, used to calculate the fluctuating vorticity and expansion ratios. It is shown in Fig. 9 that only increasing the order of accuracy of the calculation of the right-hand side of the Poisson equations significantly reduces the error of the simulation. High-order-accurate values of the source-domain velocity gradients are indispensable for the proposed splitting technique, especially when a significant difference in magnitude of the aerodynamic and acoustic fluctuations is expected.

A last analysis of this confined test case involves the effects of random perturbations on the total fluctuating-velocity field. The source-region simulations indeed often contain low-amplitude, quasi-random, high-frequency oscillations originating from the presence of numerical errors and small-scale turbulence. For this reason, a random field is superimposed onto the total velocity fluctuations, for which the amplitude of the random distortion is varied between 0.1 and 50% of the acoustic velocity amplitude ($A_{ac} = A_t = 1$). The results of these simulations are shown in Fig. 10.

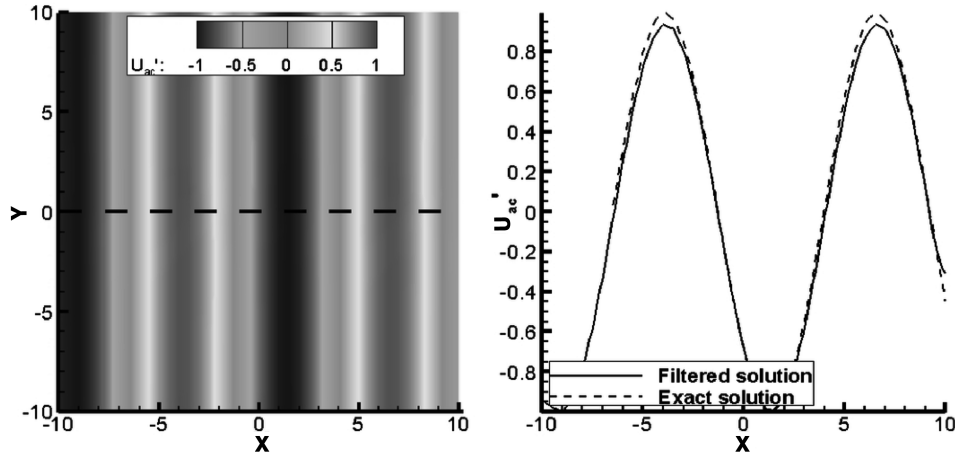


Fig. 6 Filtered acoustic velocity fluctuations u'_{ac} in the x direction; contour plot (left) and velocity along line $y = 0.0$ (right) at time step 4.000; $A_{ac} = A_t = 1$.

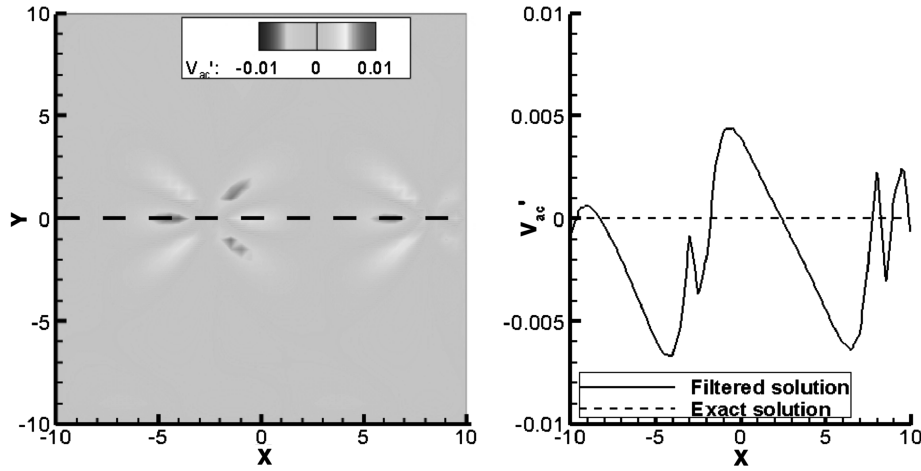


Fig. 7 Filtered acoustic velocity fluctuations v'_{ac} in the y direction; contour plot (left) and velocity along line $y = 0.0$ (right) at time step 4.000; $A_{ac} = A_t = 1$.

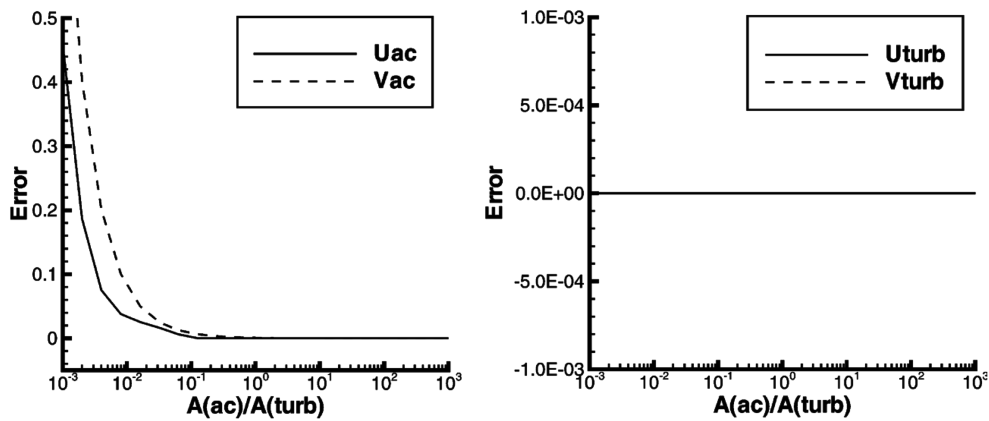


Fig. 8 Error of the acoustic (left) and aerodynamic (right) velocity fields for different values of A_{ac}/A_t .

The errors for both the filtered aerodynamic and acoustic fluctuating fields remain fairly low up to random fluctuations of 10% of the acoustic velocity amplitude A_{ac} , indicating that the proposed filtering technique is relatively insensitive to this kind of distortion in the source-domain results.

B. Free-Field Test Case

The previous test case is carried out for a confined environment, for which the mode-matching strategies can, in principle, still be used

if the acoustic perturbations are of sufficiently high amplitude and if no strong vortical outflow is occurring. An advantage of the aerodynamic/acoustic splitting technique is the fact that no assumptions toward the acoustic modes are made, and thus the filtering method can also be applied for free-field applications.

For this validation, an acoustic dipole field is calculated with the LEE [29], with a fluctuating force excitation

$$f_x = A_{ac} \cos(\pi x) \exp(-\alpha y^2) \sin(\omega t) \quad (20)$$

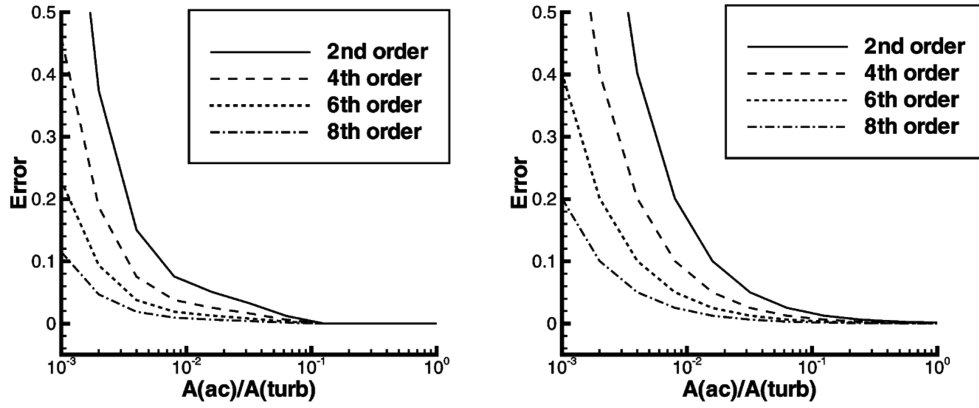


Fig. 9 Error of the acoustic x and y velocity fields u_{ac} (left) and v_{ac} (right) for different values of A_{ac}/A_t and different orders of accuracy of the right-hand-side terms.

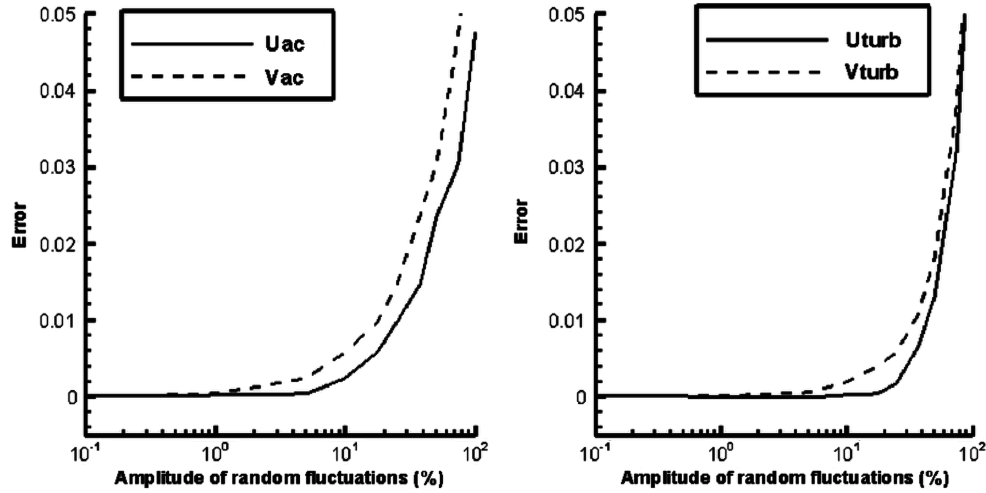


Fig. 10 Error of the acoustic (left) and aerodynamic (right) velocity fields for different values of random distortion added to the total velocity fluctuations.

with amplitude $A_{ac} = 1$, $\alpha = \ell_n 2/0.5$ and a Strouhal number of 1.5, inserted at the center of the domain. As with the confined-flow validation, a train of vortices is superimposed on this acoustic field. The total computational domain has a nondimensional length and height of 15 and the filtering region has a length and height of, respectively, 1 and 4, starting at the nondimensional x position 3, as shown in Fig. 11. The Kirchhoff surface is located at the nondimensional x position 3.6 and has a height of 15. The filtering region only covers a part of the Kirchhoff surface, because it can be assumed that the fluctuating variables above and below the filtering region only contain an acoustic fluctuating part.

The ratio A_{ac}/A_t is not varied for this test case. It is shown for the confined problem that the filtering procedure is capable of reconstructing the acoustic and aerodynamic velocity fields for any ratio of A_{ac}/A_t , as long as the right-hand side of the Poisson equations are accurately predicted. Because the same numerical procedure is used for the current test case, it can be expected that the same conclusion holds. A detailed analysis of the ratio A_{ac}/A_t for this test problem thus only gives information about the accuracy with which the expansion ratio and the vorticity field are calculated.

The mean flow is taken uniform over the whole domain, with a Mach number equal to 0.3. The vortices with amplitude $A_t = 1$ are alternately inserted and convected with the uniform mean flow at nondimensional y positions of $+0.75$ and -0.75 , with a distance in the x direction of 1 between two vortices along a constant y line. The resulting pressure field is shown in Fig. 11, in which it is clear that pressure fluctuations in the outflow region contain a nonnegligible contribution from the hydrodynamic pressure fluctuations caused by the vortical fluid motion.

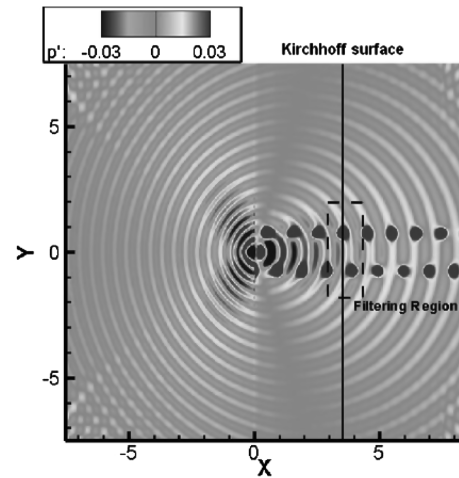


Fig. 11 Instantaneous total pressure contours p' for a dipole source with a train of vortices superimposed; filtering region (dashed line) and Kirchhoff surface (solid line).

The filtering region contains 20×300 elements with a mesh spacing of 0.05, and the simulation is carried out over 10,000 time steps with a CFL number of 1.0. To investigate the influence of interpolation errors introduced when using a different mesh for the source domain and the acoustic-propagation-region simulations, an error is introduced by the interpolation of the LEE results to the mesh

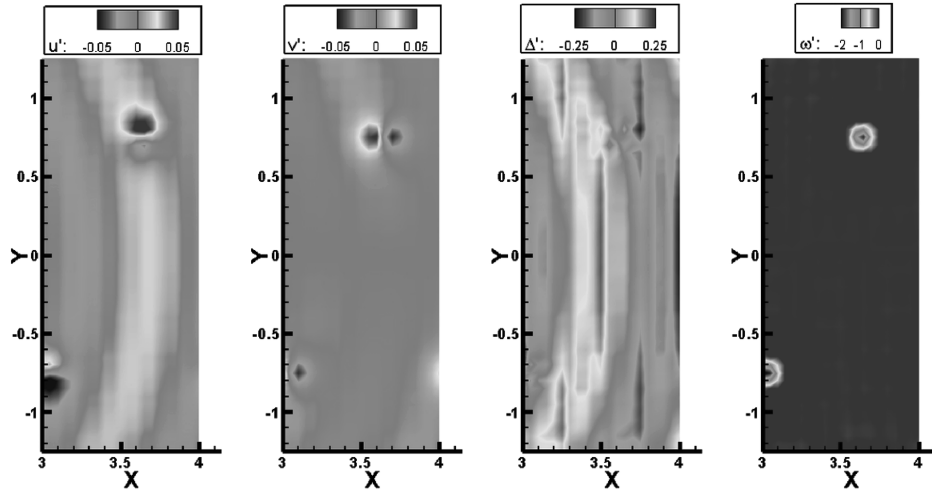


Fig. 12 Total velocity fluctuations u' (left) and v' (middle left), expansion ratio Δ' (middle right), and vorticity ω' (right) at time step 7.500 inside the filtering region.

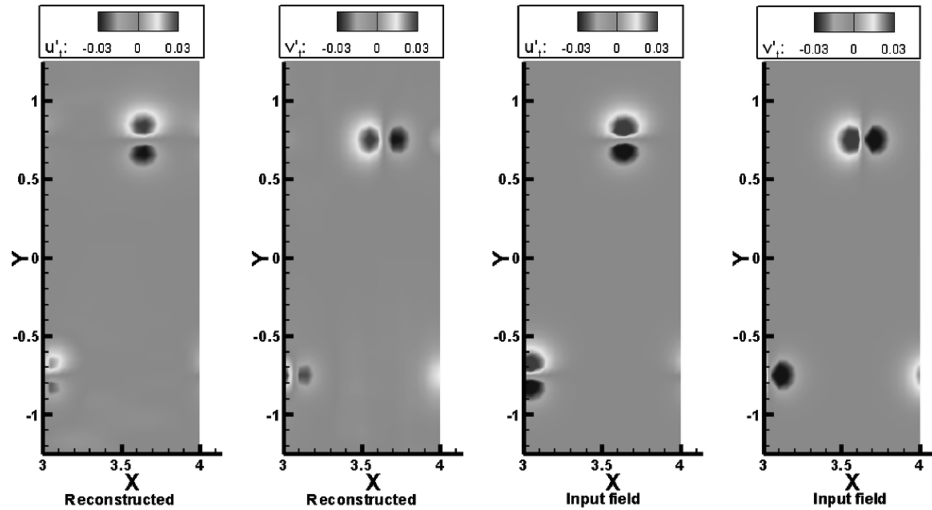


Fig. 13 Comparison between filtered u'_i (left) and v'_i (middle left) and input u'_i (middle right) and v'_i (right) aerodynamic velocity fluctuations at time step 7.500 inside the filtering region.

used for the splitting techniques. This is shown in Fig. 12, in which the total velocity fluctuations, expansion ratio, and vorticity inside the filtering region are shown at time step 7.500. The nonsmooth pattern of the expansion ratio is caused by this interpolation error.

Once the boundary conditions are applied at the borders of the filtering domain (which are, in this case, all asymptotic radiation boundary conditions), the aerodynamic and acoustic fields can be obtained. Figure 13 shows a comparison between the instantaneous reconstructed aerodynamic fluctuations and those that are initially used to construct the total velocity field inside the filtering region. As with the confined test case, an accurate representation is obtained with this aerodynamic/acoustic splitting technique, and the most dominant errors are again observed close to the boundaries of the filtering region.

The filtered acoustic field, shown on the left of Fig. 14, is also reasonably well-predicted. It is even noticed that the interpolation errors shown on the right of Fig. 14 are smoothed out by the splitting technique. This is caused by the fact that the numerical finite difference method is not able to accurately reconstruct this high-frequency behavior, and thus an additional numerical smoothing is noticed. As with the confined-flow test case, numerical errors are most apparent in the acoustic velocities in the y direction, because they have the lowest amplitude.

It is shown in the theoretical description of the splitting technique that the acoustic velocity fluctuations can be used in a second step to obtain the acoustic (and aerodynamic) pressure fluctuations inside

the filtering region, as illustrated in Fig. 15. Although the presence of hydrodynamic pressure fluctuations caused by the passing vortices is noticed in the total fluctuating pressure field, the aerodynamic/acoustic splitting technique is able to separate both fluctuating fields in an accurate way. From this figure, it is noticed (as for the confined test case) that the main errors are occurring in the vicinity of the boundaries and near locations at which one of the two fluctuating fields shows a maximum value.

The filtered acoustic variables are finally used as coupling information for the acoustic continuation of the source-region simulation with the use of the LEE as propagation equations. The Kirchhoff surface, shown in Fig. 11, is a line parallel to the y direction at a nondimensional x coordinate of 3.6. A comparison between the total and filtered acoustic and aerodynamic pressure fluctuations on the right of the Kirchhoff surface is shown in Fig. 16. From this figure, it is clear that the aerodynamic and acoustic fields are accurately separated.

In Fig. 17, different hybrid results obtained with the filtered and unfiltered acoustic information combined with the LEE and the Kirchhoff integral methods are compared with the expected acoustic solution of the dipole radiation on a data surface at a nondimensional x position of 6.0. The unfiltered hybrid results obtained with the LEE show the presence of the hydrodynamic pressure fluctuations when the vortices pass the data surface. Because the LEE support the convective propagation of hydrodynamic pressure fluctuations, the results are only incorrect in the vicinity of the vortices. The use of

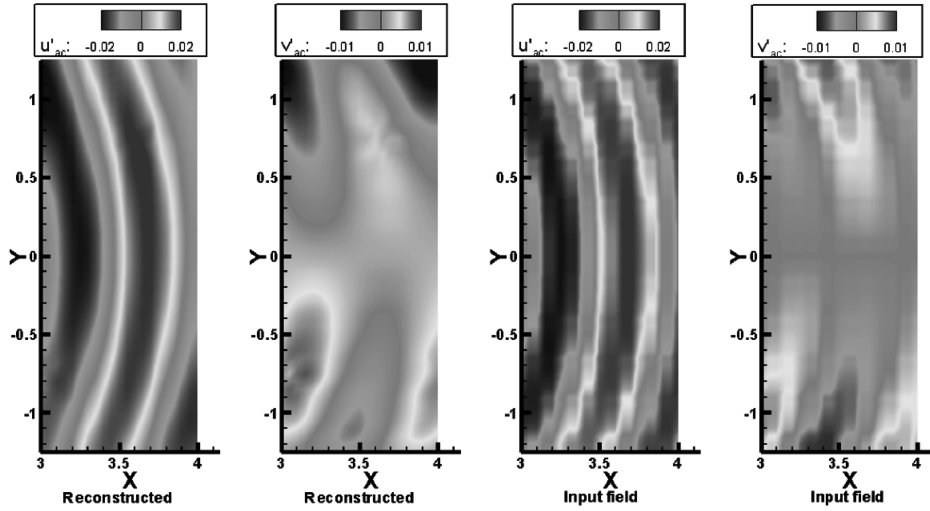


Fig. 14 Comparison between filtered u'_{ac} (left) and v'_{ac} (middle left) and input u'_{ac} (middle right) and v'_{ac} (right) acoustic velocity fluctuations at time step 7.500 inside the filtering region.

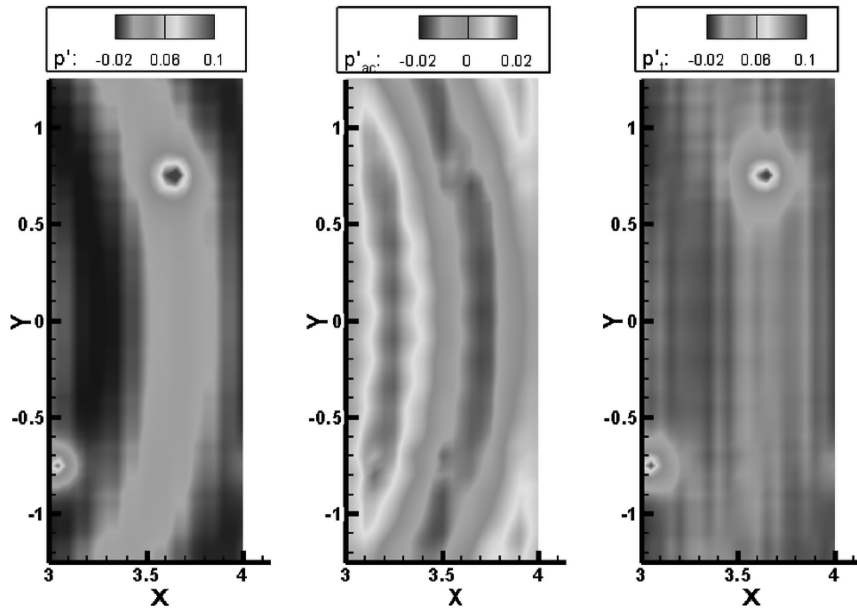


Fig. 15 Comparison between the total p' (left), acoustic p'_{ac} (middle), and hydrodynamic p'_t (right) pressure fluctuations at time step 7.500 inside the filtering region.

filtered data as coupling information with the LEE removes these nonacoustical pressure fluctuations completely, and an excellent agreement with the expected solution is obtained.

The Kirchhoff integral formulation does not allow the propagation of hydrodynamic pressure fluctuations. Every vortex that passes the Kirchhoff surface generates an acoustic pulse in the propagation region and, as a result, has an influence over the whole data surface. This is noticed when looking at the integral results obtained with the unfiltered data when the predicted field is erroneously predicted. When filtered data are used for the Kirchhoff formulation, the vortices are not present anymore and accurate acoustic results are obtained. The acoustic results are in good agreement with the LEE solution and the expected acoustic field.

V. Conclusions

Hybrid CAA methodologies are, at present, the most commonly used numerical prediction tools for engineering applications. The basic principle of these techniques is based on a domain decomposition into a source region and an acoustic propagation domain, which can both be solved with different equations, numerical discretization techniques, and grid sizes. The coupling

between both domains can be elaborated using acoustic analogies, in which the source region is replaced by a number of equivalent aeroacoustic sources or directly using acoustic information inside the source region as coupling information for the acoustic propagation equations.

Both coupling strategies were successfully applied by other researchers for a large number of aeroacoustic applications. However, it is shown that under certain circumstances, often occurring in confined-flow applications, neither of the coupling techniques can yield accurate results:

- 1) The equivalent source-term formulations, which are based on the fluctuating velocities inside the source domain, inevitably contain a contribution from the acoustic fluctuating part, if the source simulation is carried out in a compressible way. When the acoustic fluctuating part cannot be neglected, compared with the purely aerodynamic fluctuating part, the source-term formulations are no longer an accurate representation of the true aerodynamic noise sources. This is the case when acoustic resonances are excited or when a flow-acoustic feedback coupling occurs.

- 2) Acoustic continuation of the source-region simulation yields inaccurate results when a vortical outflow through the Kirchhoff surface is occurring. In this case, hydrodynamic pressure fluctuations

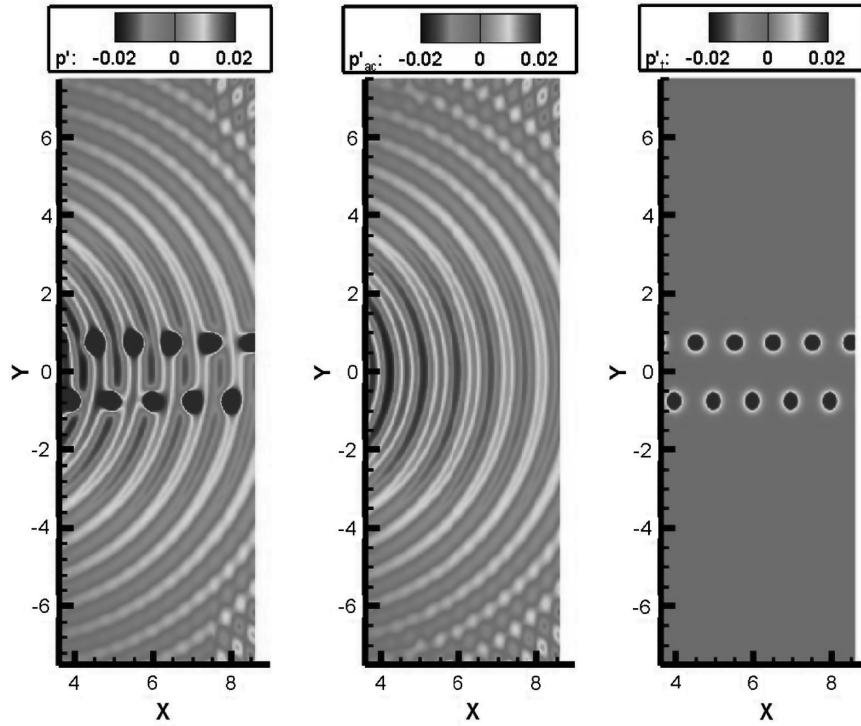


Fig. 16 Comparison between the hybrid instantaneous unfiltered (left), acoustic (middle), and aerodynamic (right) pressure fluctuations obtained with LEE and acoustic boundary conditions in the region at the right side of the Kirchhoff surface.

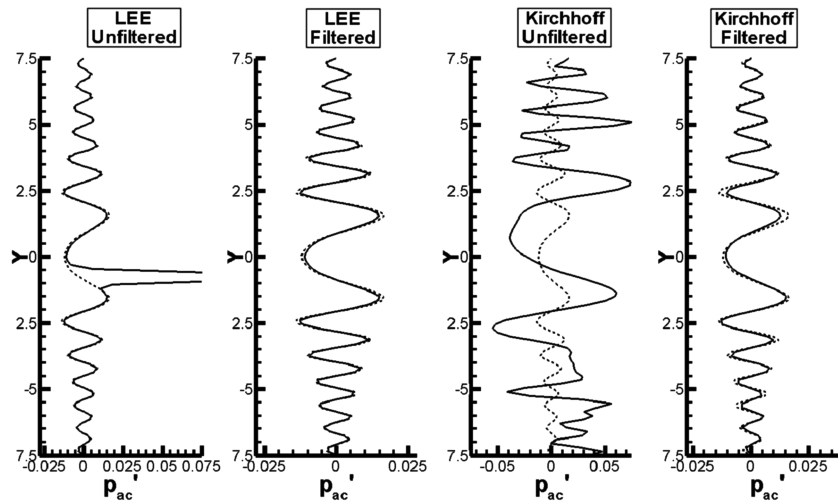


Fig. 17 Acoustic pressure at time step 7.500 on line $x = 6.0$ obtained with different filtered and unfiltered hybrid methodologies; numerical results (solid line) and reference solution (dotted line).

contaminate the final acoustic results in the outflow region. This coupling technique can thus only be used when the fluctuating values on the coupling surface contain only a contribution from the acoustic fluctuating components.

The failure of both coupling techniques illustrates the need of a splitting technique between the aerodynamic and acoustic fluctuating fields, especially for confined-flow applications. The existing mode-matching strategy based on a least-squares fit of the source-domain solution onto the acoustic duct modes is only applicable for a limited number of applications in which no vortical outflow occurs and the duct is only slowly varying in cross section. This technique only allows us to obtain acoustic pressure fluctuations and, as a result, can only be used for a coupling strategy based on an acoustic continuation of the source-region simulation, which typically has a much larger sensitivity toward the source-region results than with the equivalent sources coupling technique.

For this reason, a new aerodynamic/acoustic splitting technique is developed and validated for a number of simple academic test cases.

Because the filtering technique is based on an incompressible aerodynamic field assumption, it allows low-Mach-number applications to separate the aerodynamic and acoustic fluctuating-velocity fields by means of a system of Poisson equations, using the fluctuating expansion ratio and vorticity of the source-region simulation as source terms for, respectively, the acoustic and aerodynamic fields. The splitting technique assumes that all compressible effects are caused by the irrotational acoustic velocity field and, as a consequence, all rotational movement of the flowfield is described by the incompressible aerodynamic field. The splitting procedure involves solving the system of Poisson equations at every time step.

Some simple validations of this filtering technique show that the proposed method is generally applicable and can be combined with both coupling strategies. Furthermore, the aerodynamic/acoustic splitting technique is easy to incorporate into a flow-domain solver, because it is based on a time-domain formulation and is straightforward to implement using finite difference, finite volume,

or finite element techniques. A first study, using a finite difference implementation, shows that the method is relatively insensitive to interpolation errors between the source and the acoustic domain mesh or by the presence of a random distortions. The main source of inaccuracy of the splitting technique is caused by the boundary-condition implementation and the differentiation errors introduced by the calculation of the right-hand-side terms: the fluctuating vorticity and expansion ratio. When these numerical errors become of the same order of magnitude as the aerodynamic or acoustic fluctuating field, the splitting technique fails in accurately separating both fields.

The filtering technique can be used to investigate aerodynamically generated noise for confined-flow applications such as expansion chambers or converging-diverging nozzles (which are commonly installed in, for example, automotive exhaust systems or HVAC ducts), in which the flowfield typically has a Mach number below 0.3. Another potential application is the numerical prediction of jet noise radiation in the downstream direction, because an initially high-Mach-number jet can be considered to be incompressible at sufficiently large downstream distances from the jet potential core. To predict the far-field noise radiation using the Kirchhoff method or the Ffowcs-Williams/Hawkings technique, a control surface that cuts across the jet flow is needed. In this downstream region, the proposed splitting technique can, as with the free-field test case presented in this paper, be used to separate the acoustic fluctuations from the hydrodynamic fluctuations, resulting in more accurate coupling information on the control surface that is being penetrated by turbulence.

Until applied to some of the preceding three-dimensional simulations mentioned, it is hard to predict the limitations of the aerodynamic/acoustic splitting technique, such as the influence of the accuracy of the source-domain simulation, the sensitivity toward the ratio of acoustic fluctuations to aerodynamic fluctuations on the filtering procedure, or the Mach number range for which this technique can be used. However, it can be expected that this splitting procedure allows us to broaden the applicability range and accuracy of hybrid CAA methodologies and to gain more insight into noise-generating mechanisms.

Acknowledgments

The authors want to acknowledge the financial support given by the Research Foundation of Flanders (FWO G.0467.05) and the Institute for the Promotion of Innovation by Science and Technology in Flanders (SBO-IWT 05.0163).

References

- [1] Colonius, T., Lele, S. K., and Moin, P., "Boundary Conditions for Direct Computation of Aerodynamic Sound Generation," *AIAA Journal*, Vol. 31, No. 9, 1993, pp. 1574–1582.
- [2] Mitchell, B. E., Lele, S. K., and Moin, P., "Direct Computation of the Sound from a Compressible Co-Rotating Vortex Pair," *Journal of Fluid Mechanics*, Vol. 285, No. 1, 1995, pp. 181–202. doi:10.1017/S0022112095000504
- [3] Gloerfelt, X., Bailly, C., and Juvé, D., "Direct Computation of the Noise Radiated by a Subsonic Cavity Flow and Application of Integral Methods," *Journal of Sound and Vibration*, Vol. 266, No. 1, 2003, pp. 119–146. doi:10.1016/S0022-460X(02)01531-6
- [4] Tam, C. K. W., "Computational Aeroacoustics: Issues and Methods," *AIAA Journal*, Vol. 33, No. 10, 1995, pp. 1788–1796.
- [5] Goldstein, M. E., *Aeroacoustics*, McGraw-Hill, New York, 1976.
- [6] Bailly, C., and Juvé, D., "Numerical Solution of Acoustic Propagation Using Linearized Euler Equations," *AIAA Journal*, Vol. 38, No. 1, 2000, pp. 22–29.
- [7] Ewert, R., and Schröder, W., "Acoustic Perturbation Equations Based on Flow Decomposition via Source Filtering," *Journal of Computational Physics*, Vol. 188, No. 2, 2003, pp. 365–398. doi:10.1016/S0021-9991(03)00168-2
- [8] Seo, J. H., and Moon, Y. J., "Linearized Perturbed Compressible Equations for Aeroacoustic Noise Prediction at Low Mach Numbers," *Journal of Computational Physics*, Vol. 218, No. 2, 2006, pp. 702–719. doi:10.1016/j.jcp.2006.03.003
- [9] Lighthill, M. J., "On Sound Generated Aerodynamically, 1: General Theory," *Proceedings of the Royal Society of London A*, Vol. 211, No. 1107, 1952, pp. 564–587. doi:10.1098/rspa.1952.0060
- [10] Lighthill, M. J., "On Sound Generated Aerodynamically, 2: Turbulence as a Source of Sound," *Proceedings of the Royal Society of London A*, Vol. 222, No. 1148, 1954, pp. 1–32. doi:10.1098/rspa.1954.0049
- [11] Curle, N., "The Influence of Solid Boundaries on Aerodynamics Sound," *Proceedings of the Royal Society of London A*, Vol. 231, No. 1187, 1955, pp. 505–514. doi:10.1098/rspa.1955.0191
- [12] Ffowcs-Williams, J. E., and Hawkings, D. L., "Sound Generation by Turbulence and Surfaces in Arbitrary Motion," *Proceedings of the Royal Society of London A*, Vol. 264, No. 1151, 1969, pp. 321–342. doi:10.1098/rsta.1969.0031
- [13] Powell, A., "Theory of Vortex Sound," *Journal of the Acoustical Society of America*, Vol. 36, No. 1, 1964, pp. 177–195. doi:10.1121/1.1918931
- [14] Howe, M. S., "Contributions to the Theory of Aerodynamic Sound, with Application to Excess Jet Noise and the Theory of the Flute," *Journal of Fluid Mechanics*, Vol. 71, No. 4, 1975, pp. 625–673. doi:10.1017/S0022112075002777
- [15] Lyrintzis, A. S., "Surface Integral Methods in Computational Aeroacoustics from the (CFD) Near-Field to the (Acoustic) Far-Field," *International Journal of Aeroacoustics*, Vol. 2, No. 2, 2003, pp. 95–128. doi:10.1260/14754720322775498
- [16] Chu, B.-T., and Kovásznyai, L. S. G., "Non Linear Interactions in a Viscous Heat Conducting Compressible Gas," *Journal of Fluid Mechanics*, Vol. 3, No. 5, 1958, pp. 494–514. doi:10.1017/S0022112058000148
- [17] Möhring, W., "On Vortex Sound at Low Mach Number," *Journal of Fluid Mechanics*, Vol. 85, No. 4, 1978, pp. 685–691. doi:10.1017/S0022112078000865
- [18] De Roeck, W., Rubio, G., Baelmans, M., Sas, P., and Desmet, W., "The Influence of Flow Domain Modelling on the Accuracy of Direct and Hybrid Aeroacoustic Noise Calculations," *AIAA Paper 2006-2419*, 2006.
- [19] Freund, J. B., Lele, S. K., and Moin, P., "Calculation of the Radiated Sound Field Using an Open Kirchhoff Surface," *AIAA Journal*, Vol. 34, No. 5, 1996, pp. 909–916.
- [20] Ovenden, N. C., and Rienstra, S. W., "Mode-Matching Strategies in Slowly Varying Engine Ducts," *AIAA Journal*, Vol. 42, No. 9, 2004, pp. 1832–1840.
- [21] Rienstra, S. W., "Sound Propagation in Slowly Varying Lined Flow Ducts of Arbitrary Cross Section," *Journal of Fluid Mechanics*, Vol. 495, Nov. 2003, pp. 157–173. doi:10.1017/S0022112003006050
- [22] Rienstra, S. W., "Sound Transmission in Slowly Varying Circular and Annular Lined Ducts with Flow," *Journal of Fluid Mechanics*, Vol. 380, Feb. 1999, pp. 279–296. doi:10.1017/S0022112098003607
- [23] De Roeck, W., Rubio, G., and Desmet, W., "On the Use of Filtering Techniques for Hybrid Methods in Computational Aero-Acoustics," *ISMA 2006 [CD-ROM]*, Katholieke Univ. Leuven, Leuven, Belgium, 2006.
- [24] Wang, M., Lele, S. K., and Moin, P., "Computation of Quadrupole Noise Using Acoustic Analogy," *AIAA Journal*, Vol. 34, No. 11, 1996, pp. 2247–2256.
- [25] Shur, M. L., Spalart, P. R., and Strelets, M. K., "Noise Prediction for Increasingly Complex Jets, Part 1: Methods and Tests," *International Journal of Aeroacoustics*, Vol. 4, No. 3, 2005, pp. 213–246. doi:10.1260/1475472054771376
- [26] Batchelor, G. K., *An Introduction to Fluid Dynamics*, Cambridge Univ. Press, Cambridge, England, U.K., 1967.
- [27] Tam, C. K. W., and Dong, Z., "Radiation and Outflow Boundary Conditions for Direct Computation of Acoustic and Flow Disturbances in a Nonuniform Mean Flow," *Journal of Computational Acoustics*, Vol. 4, No. 2, 1996, pp. 175–201. doi:10.1142/S0218396X96000040
- [28] Ferziger, J., and Perić, M., *Computational Methods for Fluid Dynamics*, Springer-Verlag, Berlin, 1996.
- [29] De Roeck, W., "Hybrid Methodologies for the Computational Aeroacoustic Analysis of Confined, Subsonic Flows," Ph.D., Thesis, Katholieke Univ. Leuven, Leuven, Belgium, 2007.